

Mesoscopic inhomogeneities in concentrated electrolytes

O. Patsahan

*Institute for Condensed Matter Physics of the National
Academy of Sciences of Ukraine, Lviv, Ukraine*

A. Ciach

Institute of Physical Chemistry, Polish Academy of Sciences, 01-224 Warszawa, Poland

(Dated: September 29, 2021)

Abstract

A mesoscopic theory for water-in-salt electrolytes combining density functional and field-theoretic methods is developed in order to explain the unexpectedly large period of the oscillatory decay of the disjoining pressure observed in recent experiments for the LiTFSI (lithium bis(trifluoromethylsulfonyl)-imide) salt [T. S. Groves et. al., J. Phys. Chem. Lett. **12**, 1702 (2021)]. We assumed spherical ions with different diameters, and implicit solvent inducing strong, short-range attraction between ions of the same sign. For this highly simplified model, we calculated correlation functions. Our results indicate that mesoscopic inhomogeneities can occur when the sum of the Coulomb and the water-mediated interactions between like ions is attractive at short- and repulsive at large distances. We adjusted the attractive part of the potential to the water-in-LiTFSI electrolyte, and obtained both the period and the decay rate of the correlations in a semiquantitative agreement with the experiment. In particular, the decay length of the correlations increases nearly linearly with the volume fraction of ions.

I. INTRODUCTION

For many years it was commonly assumed that dilute electrolytes, very well described by the Debye-Hückel (DH) theory, are more suitable for electrochemical devices than the concentrated ones. For this reason, neither experimentalists nor theoreticians paid much attention to the concentrated electrolytes. Recently, however, it was noted that the concentrated electrolytes have advantages such as a large electrochemical stability window and they may find applications in electrochemical devices, for example in lithium ion batteries [1–4]. These observations motivated intensive experimental studies. It was found that when the concentration of ions, ρ , increases, the deviation between experimental results and predictions of the DH theory becomes very large. Even qualitative trends well documented for the dilute electrolytes, such as decreasing screening length with increasing ρ , are opposite in concentrated electrolytes and ionic liquids (IL) solutions. Recent surface-force balance (SFB) experiments show that in the above systems, the screening length λ_s is proportional to ρ , while the Debye screening length λ_D perfectly describing the dilute electrolytes is proportional to $1/\sqrt{\rho}$. The scaling behavior $\lambda_s/\lambda_D \sim (a/\lambda_D)^3$, where a is the average diameter of the ions, was found for a number of concentrated solutions of simple salts in water, IL solutions and alkali halide solutions [5–7]. This universal behavior suggests that the observed decay of the disjoining pressure does not depend on specific interactions, but only on the Coulomb potential that is common for all the studied systems.

The strong disagreement of experimental results for concentrated electrolytes with the DH theory predictions attracted attention of theoreticians, but despite significant effort in theoretical and simulation studies, the experimental results are not fully explained yet [8–17]. In several theories and simulation studies the scaling behavior $\lambda_s/\lambda_D \sim (a/\lambda_D)^\alpha$ was found, but the scaling exponent as well as λ_s in these studies were significantly smaller than in the experiments [10–14, 16, 17]. Correct scaling for the charge-charge correlation length (that should be equal to λ_s) was obtained in [18], where it was shown that the local variance of the charge density plays a significant role for large concentrations of ions. However, oscillatory decay obtained in the theory is at variance with the asymptotic monotonic decay of the disjoining pressure observed in the experiments [4–7].

Theoretical studies of ionic systems are very often based on the restricted primitive model (RPM) [19, 20]. In the RPM, the ions are treated as charged hard spheres with the same

diameter, and the Coulomb potential between the ions is assumed. The solvent, however, is treated as a dielectric continuum. The charge-charge correlations in the RPM decay monotonically in dilute systems, and exhibit exponentially damped oscillations for large ρ [21, 22]. More precisely, the oscillatory decay of charge-charge correlations occurs on the large-density side of the so called Kirkwood line [23] on the (ρ, T) diagram. For the charge density profile near a planar electrode, as well as for the disjoining pressure between parallel planar electrodes, the decay length and the period of oscillations are expected to be the same as the corresponding length in the charge-charge correlation function in the bulk electrolyte at the same thermodynamic state. The period of oscillations is close to $2a$ [21, 22], showing that the neighborhood of opposite charges is more probable than the neighborhood of like charges. The observed difference from the random distribution of charges is expected by the requirement of local charge-neutrality. The predictions concerning the period of the damped oscillations were verified by simulations and experiments [6, 7, 17, 24, 25]. The decay length of the correlations in the RPM, however, depends on the approximation used in theoretical studies and remains a question of a debate [18, 21, 26]. In the SFB experiments, the oscillatory decay of the disjoining pressure was observed up to some distance between the crossed mica cylinders, but the asymptotic decay at larger distances was monotonic [5–7].

Strong disagreement with the RPM predictions was observed in recent SFB experiments for concentrated LiTFSI (lithium bis(trifluoromethylsulfonyl)-imide) in water [4]. It was found that the period of oscillations of the disjoining pressure was twice as large as the sum of diameters of the cation and the anion, observed previously in many concentrated electrolytes and predicted by the RPM. The same length scale of inhomogeneities in the bulk was observed in scattering experiments for concentrated LiTFSI [3]. At large distances, the decay of the disjoining pressure changes from oscillatory to monotonic, as found before for the other systems. Importantly, the decay length increases with increasing salt concentration and is of the same order of magnitude as observed previously in various concentrated electrolytes [4].

In the LiTFSI salt, the size and the chemical properties of the TFSI⁻ and Li⁺ ions are significantly different [3]. The TFSI⁻ ion is not spherical, and is much larger than the Li⁺ ion. Moreover, the Li⁺ ions are very well solvated in water, in contrast to the hydrophobic TFSI⁻ ions. Based on the above observations, we conclude that in the above water-in-salt electrolyte the size difference between the ions, and/or the specific non-Coulombic interactions must play a significant role, and cannot be neglected.

The effect of specific interactions was studied in the RPM supplemented with additional short-range (SR) interactions in Ref.[27]. On the other hand, the size difference between the ions with neglected SR (primitive model, (PM)) was studied in Refs.[28–31]. It was found that the length scale of inhomogeneities depended on the strength of the SR interactions, and on the size asymmetry. These general predictions were not verified by experiments, however. In the particular case of LiTFSI, the question of the origin of the scale of inhomogeneities and of the range of correlations is open.

In this work we develop a minimal model for the water-in-salt electrolyte, and fit the parameters to the particular case of the LiTFSI salt. The minimal model can allow to see which details of the system properties can be neglected without changing the key features of the decay of the correlations. The important questions are: (i) to what extent properties of the systems with large size asymmetry of ions and with strong specific interactions depend on details of the interactions and on the geometry of the ions? (ii) can the solvent be treated as a dielectric continuum that mediates effective ion-ion interactions, or must it be taken into account explicitly? (iii) what types of approximations should be used to compute the correlation functions reproducing the qualitative trends found in experiments?

In our model we assume that both, the size difference and the effective SR interactions between the ions must be taken into account. The solvent, however, can be treated as a dielectric continuum. We further assume that water induces effective ion-ion interactions of a range much shorter than the range of the Coulomb potential. The model is introduced in sec.II. In sec.III we develop an approximate form of the grand-thermodynamic potential functional of local ionic densities that allows to obtain correlation functions. In sec.IV we calculate the correlation functions first in mean-field approximation (sec.IV A), and next beyond MF, using the procedure developed in [32, 33] (sec.IV B). We obtain a semi-quantitative agreement with experiment when we assume strong water-induced short-range attraction between the cations. The last section contains our conclusions.

II. CONSTRUCTION OF THE THEORETICAL MODEL

In this section, we describe the assumptions and the approximations leading to the effective specific interactions between the ions in the LiTFSI salt dissolved in water. We take into account the ionic sizes reported in Ref. [4]. In addition, we develop the approximation

for the SR interactions based on the requirement that the model predicts inhomogeneities at the length scale $\sim 2(\sigma_+ + \sigma_-) = 4a$, where σ_{\pm} denotes the diameter of the corresponding ion. Once the form of the SR interactions is assumed, we calculate the correlation functions for different volume fractions of ions without further fitting of any parameters, using the method summarized in sec.III.

We first consider the excluded-volume interactions. The TFSI⁻ ions are much bigger than the Li⁺ ions, and have a shape of an ellipsoid. We assume that the size difference is more important than the non-spherical shape, and assume that the Li⁺ and TFSI⁻ ions can be modeled as charged hard spheres with the diameter $\sigma_+ = 0.2nm$ and $\sigma_- = 0.6nm$, respectively.

From the previous studies [3] we know that the Li⁺ ions are strongly hydrophilic, while the TFSI⁻ ions are strongly hydrophobic. The Li⁺ ions are solvated by water, and the TFSI⁻ ions are not. This means that the short-range non-Coulombic forces have a strong effect on the distribution of the ions, and cannot be neglected. Even though the water- Li⁺ interactions play an important role, we assume that water can be treated as a dielectric continuum, as in the PM and the classical DH theory. We assume, however that water molecules mediate effective interactions between the Li⁺ ions, and that these solvent-induced effective interactions are short-ranged (compared to the Coulomb potential) but strong. In addition, we assume short-ranged interactions between the TFSI⁻ ions, but neglect the interactions between the Li⁺ and TFSI⁻ ions other than the Coulomb potential. We do not attempt to determine the precise shape of these interactions, because the correlations at large distances depend only on some gross features of the potentials, such as their range and strength. This is because in collective phenomena involving many ions and solvent molecules, many details are washed out by averaging over all distributions of the ions and the solvent molecules.

With the above assumptions, we model the aqueous electrolyte solution as a binary mixture of oppositely charged hard spheres of different diameters ($\sigma_+ \neq \sigma_-$) immersed in structureless dielectric medium with the dielectric constant ε . We limit ourselves to the model with monovalent ions ($z_+ = z_- = 1$). The presence of the solvent is taken into account through the solvent-induced effective short-range attractive interactions between the ions of the same sign. Therefore, we assume that the pair interaction potentials between two ions for $r > \sigma_{\alpha\beta} = (\sigma_{\alpha} + \sigma_{\beta})/2$, with $\alpha = +, -$ and $\beta = +, -$, can be presented in the

form:

$$U_{\alpha\beta}(r) = U_{\alpha\beta}^C(r) + U_{\alpha\beta}^A(r). \quad (1)$$

Here, $U_{\alpha\beta}^C(r)$ are the Coulomb potentials between the ions with the signs α and β . As a length unit we choose the sum of radii, $a = (\sigma_+ + \sigma_-)/2$. The Coulomb potentials for $r^* \equiv r/a$ are

$$\beta U_{++}^C(r^*) = \frac{l_B \theta(r^* - a_+)}{r^*}, \quad (2)$$

$$\beta U_{--}^C(r^*) = \frac{l_B \theta(r^* - a_-)}{r^*}, \quad (3)$$

$$\beta U_{+-}^C(r^*) = -\frac{l_B \theta(r^* - 1)}{r^*}, \quad (4)$$

where $a_{\pm} = \sigma_{\pm}/a$,

$$l_B = \frac{1}{T^*} = \beta E_C, \quad E_C = \frac{e^2}{a\epsilon}, \quad (5)$$

and $\beta = 1/k_B T$ with k_B and T denoting the Boltzmann constant and temperature, respectively. l_B is the Bjerrum length in a units, E_C is the electrostatic potential of the pair of oppositely charged ions at contact, and the reduced temperature T^* is in units of E_C . The unit step function $\theta(x) = 1$ for $x > 0$ and $\theta(x) = 0$ for $x < 0$, prevents from contributions to the electrostatic energy of the pair of ions that would come from forbidden overlap of the hard cores.

For $U_{\alpha\alpha}^A(r)$ we assume a short-range attractive potential. The form of the sum of the direct (van der Waals type) and solvent-induced interactions is unknown, but we assume that its detailed shape is not necessary for studies of the collective phenomena such as the long-distance correlations. For simplicity of calculations, we assume the attractive Yukawa potentials for $U_{\alpha\alpha}^A(r)$,

$$\beta U_{\alpha\alpha}^A(r^*) = -l_B \epsilon_{\alpha\alpha}^* a_{\alpha} \frac{e^{-z_{\alpha}^*(r^* - a_{\alpha})}}{r^*} \theta(r^* - a_{\alpha}), \quad \alpha = +, -, \quad (6)$$

where z_{α}^* is in the a^{-1} units, and we assume that $z_+^* = z_-^* = z = 1.8$ to assure fast decay of these interactions. $\epsilon_{\alpha\alpha}^*$ measures the strength of the effective non-Coulombic interactions in units of E_C . Introducing the size-asymmetry parameter

$$\delta = \frac{\sigma_- - \sigma_+}{\sigma_- + \sigma_+} \quad (7)$$

we get $a_{\pm} = 1 \mp \delta$.

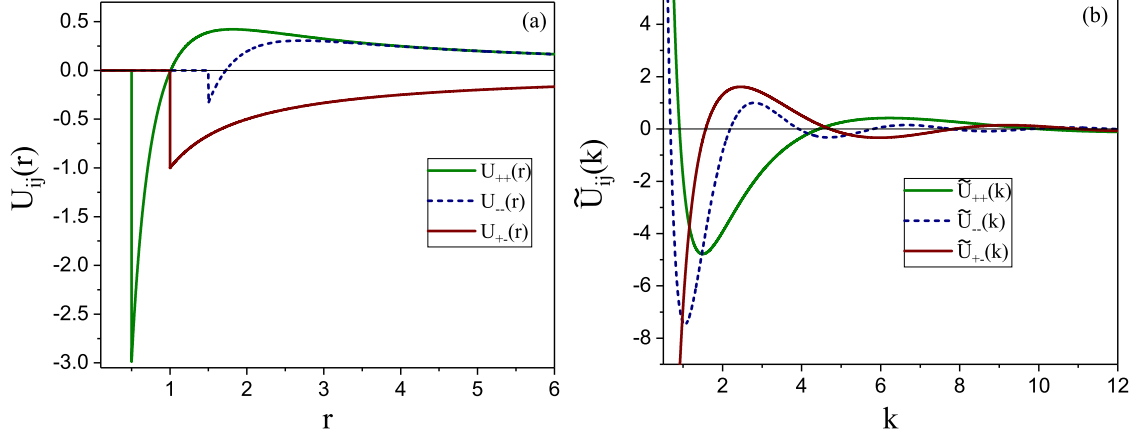


FIG. 1: The interaction potentials $U_{\alpha\beta}(r)$ (Eqs.(1)-(6)) for the model with $\delta = 0.5$, $\epsilon_{++}^* = 5$, and $\epsilon_{--}^* = 1$ in real space (a) and in Fourier representation (b). $U_{\alpha\beta}$ are in units of E_C . E_C and δ are defined in (5) and (7). r and k are in a and a^{-1} units, respectively, where $a = (\sigma_+ + \sigma_-)/2$.

It remains to adjust the parameters $\epsilon_{\alpha\alpha}^*$ to particular ions. We assume that for the TFSI⁻ ions $\epsilon_{--}^* = 1$, and treat ϵ_{++}^* as a fitting parameter. In order to find the best approximation for the Li⁺ ions in water, we calculate the length scale of inhomogeneities for arbitrary ϵ_{++}^* in sec.IV A. We find that $\epsilon_{++}^* = 5$ leads to a satisfactory agreement of the length scale of inhomogeneities with the experimental results. Based on this observation, we assume $\epsilon_{++}^* = 5$ for the considered system. Note that the second important length scale, λ_s , will be determined for several concentrations of ions without additional fitting.

In Fig. 1 (a) the potentials $U_{\alpha\beta}(r)$ normalized by $E_C = e^2/(a\epsilon)$ are shown for the model with $\epsilon_{++}^* = 5$, $\epsilon_{--}^* = 1$ and $\delta = 0.5$. For the chosen parameters, the interaction potentials between like ions consist of short-range attraction (SA) and electrostatic long-range repulsion (LR). Competing interaction potentials of this kind are also known as SALR potentials. In one-component systems, the SALR-type interactions can lead to spontaneously formed stable aggregates of particles, such as spherical or elongated clusters, networks or layers [34–36]. The Fourier transforms of the potentials $U_{\alpha\beta}(r)/E_c$ for the above mentioned model are shown in Fig. 1 (b), and the corresponding expressions are given in Appendix A. It is seen that $\tilde{U}_{++}(k)$ and $\tilde{U}_{--}(k)$ take minima at $k \neq 0$ which are rather close to each other.

III. THEORETICAL FORMALISM: A BRIEF SUMMARY

In this section we present a brief description of the mesoscopic theory for inhomogeneous mixtures [32, 37]. In this theory, mesoscopic regions and mesoscopic states are considered. In a particular mesoscopic state, the volume fraction of ions with the α sign around the point \mathbf{r} , $\zeta_\alpha(\mathbf{r})$, is the fraction of the volume of the mesoscopic region occupied by this type of ions. The mesoscopic regions are comparable with or larger than 1 (in a -units), and smaller than the scale of the inhomogeneities. The functions $\zeta_\alpha(\mathbf{r})$ representing the local volume fraction can be considered as constraints imposed on the microscopic states. The local volume fraction of ions is given by $\zeta(\mathbf{r}) = \zeta_+(\mathbf{r}) + \zeta_-(\mathbf{r})$. $\zeta(\mathbf{r})$ averaged over the system volume is denoted by $\bar{\zeta}$.

The grand thermodynamic potential in the presence of the above mesoscopic constraints can be written in the form

$$\Omega_{co}[\zeta_+, \zeta_-] = U_{co}[\zeta_+, \zeta_-] - TS[\zeta_+, \zeta_-] - \mu_\alpha \int d\mathbf{r} \zeta_\alpha(\mathbf{r}),$$

where U_{co} , S , and μ_α are the internal energy, the entropy, and the chemical potential of the species α , respectively. Hereafter, summation convention for repeated indices is used. We make the approximation $-TS = \int d\mathbf{r} f_h(\zeta_+(\mathbf{r}), \zeta_-(\mathbf{r}))$, where $f_h(\zeta_+(\mathbf{r}), \zeta_-(\mathbf{r}))$ is the free-energy density of the hard-core reference system in the local-density approximation,

$$\beta f_h = \rho_+ \ln \rho_+ + \rho_- \ln \rho_- + \beta f_{hs},$$

where f_{hs} is the contribution to the free energy density associated with packing of hard spheres with two different diameters. The expression for f_{hs} in the Carnahan-Starling approximation is given in Appendix B.

U_{co} is given by the expression

$$U_{co}[\zeta_+, \zeta_-] = \frac{1}{2} \int_{\mathbf{r}_1} \int_{\mathbf{r}_2} V_{\alpha\beta}(|\mathbf{r}_1 - \mathbf{r}_2|) \zeta_\alpha(\mathbf{r}_1) \zeta_\beta(\mathbf{r}_2).$$

Because $\zeta_\alpha = \pi \rho_\alpha \sigma^3 / 6$ is used in the above definition, we have rescaled the interaction potential,

$$V_{\alpha\beta}(r) = \frac{U_{\alpha\beta}(r)}{v_\alpha v_\beta}, \quad v_\alpha = \pi \sigma^3 / 6. \quad (8)$$

When the constraints imposed on the microscopic states by $\zeta_+(\mathbf{r})$ and $\zeta_-(\mathbf{r})$ are released, the microscopic states incompatible with $\zeta_+(\mathbf{r})$ and $\zeta_-(\mathbf{r})$ can appear, and the grand potential

contains a fluctuation contribution and has the form [37]

$$\beta\Omega[\zeta_+, \zeta_-] = \beta\Omega_{co}[\zeta_+, \zeta_-] - \ln \left[\int D\phi_+ \int D\phi_- e^{-\beta H_{fluc}} \right], \quad (9)$$

where

$$H_{fluc} = \Omega_{co}[\zeta_+ + \phi_+, \zeta_- + \phi_-] - \Omega_{co}[\zeta_+, \zeta_-]$$

is associated with the appearance of the fluctuation ϕ_α of the local volume fraction ζ_α . In MF, the second term on the RHS of Eq.(9) is neglected.

We are interested in the correlation functions in the disordered phase

$$G_{\alpha\beta}(\mathbf{r}) = \langle \Delta\zeta_\alpha(\mathbf{r}_0) \Delta\zeta_\beta(\mathbf{r} + \mathbf{r}_0) \rangle, \quad \alpha, \beta = +, - \quad (10)$$

where $\Delta\zeta_\alpha(\mathbf{r}) = \zeta_\alpha(\mathbf{r}) - \bar{\zeta}_\alpha$, and $\bar{\zeta}_\alpha$ is the average volume fraction of the ions with the α sign. The matrix \mathbf{G} with the elements defined in (10) satisfies the analog of the Ornstein-Zernicke equation, $\mathbf{G} = \mathbf{C}^{-1}$, where the inverse correlation functions $\tilde{C}_{\alpha\beta}$ are the second functional derivatives of $\beta\Omega[\zeta_+, \zeta_-]$ with respect to ζ_α and ζ_β [37].

In the lowest-order nontrivial approximation beyond MF [32, 37],

$$\tilde{C}_{\alpha\beta}(k) = \beta\tilde{V}_{\alpha\beta}(k) + A_{\alpha\beta} + \frac{A_{\alpha\beta\gamma\delta}}{2}\mathcal{G}_{\gamma\delta}, \quad (11)$$

where $\tilde{f}(k)$ denotes the function f in Fourier representation. In the above equation,

$$A_{\alpha_1 \dots \alpha_j} = \frac{\partial^j \beta f_h(\zeta_+, \zeta_-)}{\partial \zeta_{\alpha_1} \dots \partial \zeta_{\alpha_j}}, \quad (12)$$

with $\alpha_i = +, -$. Note that in this approximation, the dependence of $\tilde{C}_{\alpha\beta}(k)$ on k comes only from $\beta\tilde{V}_{\alpha\beta}(k)$. The last term in Eq.(11) is the fluctuation contribution, and comes from the last term in (9) in the Brazovskii-type approximation [38]. Here, $\mathcal{G}_{\gamma\delta}$ denotes the integral

$$\mathcal{G}_{\gamma\delta} = \int \frac{d\mathbf{k}}{(2\pi)^3} \tilde{G}_{\gamma\delta}(k). \quad (13)$$

Eqs.(11)-(13) have to be solved self-consistently. In general, it is a nontrivial task.

Note that $\mathcal{G}_{\alpha\alpha} = \langle \Delta\zeta_\alpha(\mathbf{r}) \Delta\zeta_\alpha(\mathbf{r}) \rangle$ is a local variance of ζ_α , i.e. $\sqrt{\mathcal{G}_{\alpha\alpha}}$ is the standard deviation from the space-averaged value of the local volume fraction of the α -ions. The larger is $\mathcal{G}_{\alpha\alpha}$, the stronger are the mesoscopic inhomogeneities.

We focus on the disordered inhomogeneous phase and assume that the inhomogeneities occur on a well-defined length scale. In such a case, the peak of $\tilde{G}_{\gamma\delta}(k)$ (proportional to

the structure factor) is high and narrow. For functions with a high, narrow peak, the main contribution to the integral comes from the vicinity of the maximum. We assume that the maximum of all the integrands in (13) is very close to the minimum at $k = k_0$ of $\det \tilde{\mathbf{C}}(k)$, and we make the approximation

$$\mathcal{G}_{\alpha\beta} = [\tilde{C}_{\alpha\beta}(k_0)]\mathcal{G}, \quad (14)$$

where $[\tilde{C}_{\alpha\alpha}(k)] = \tilde{C}_{\beta\beta}(k)$ and $[\tilde{C}_{\alpha\beta}(k)] = -\tilde{C}_{\alpha\beta}(k)$ for $\alpha \neq \beta$, and

$$\mathcal{G} = \int \frac{d\mathbf{k}}{(2\pi)^3} \frac{1}{\det \tilde{\mathbf{C}}(k)}. \quad (15)$$

Near the minimum at k_0 , we have the approximation

$$\det \tilde{\mathbf{C}}(k) = D_0 + \frac{\beta \tilde{W}''(k_0)}{2}(k - k_0)^2 + \dots \quad (16)$$

where

$$D_0 = \det \tilde{\mathbf{C}}(k_0), \quad (17)$$

and $\beta \tilde{W}''(k_0)$ is the second-order derivative of $\det \tilde{\mathbf{C}}(k)$ with respect to the wave number k at $k = k_0$. From the approximation (16) and (15), we obtain [37, 39]

$$\mathcal{G} \approx \frac{k_0^2}{\pi \sqrt{2\beta \tilde{W}''(k_0) D_0}}.$$

With all the above assumptions, the problem reduces to determination of the minimum of $\det \tilde{\mathbf{C}}(k)$, and to a solution of three algebraic equations for $\tilde{C}_{\alpha\beta}(k_0)$ (see (11) and (14)) because,

$$\tilde{C}_{\alpha\beta}(k) = \tilde{C}_{\alpha\beta}(k_0) + \beta \Delta \tilde{V}_{\alpha\beta}(k), \quad \alpha, \beta = +, - \quad (18)$$

where

$$\Delta \tilde{V}_{\alpha\beta}(k) = \tilde{V}_{\alpha\beta}(k) - \tilde{V}_{\alpha\beta}(k_0) \approx \frac{V_{\alpha\beta}''(k_0)}{8k_0^2}(k^2 - k_0^2)^2. \quad (19)$$

The last approximation is valid for $k \approx k_0$.

It should be noted that the results obtained within the framework of this theory for several models of inhomogeneous mixtures were verified by simulations [32, 33, 40].

IV. RESULTS

A. MF approximation

In MF, we neglect the last term in Eq. (11), and easily obtain explicit expressions for the matrix $\tilde{\mathbf{C}}^{MF}(k)$ inverse to the matrix of correlations. These expressions are shown in Appendix C. In MF, the disordered phase becomes unstable with respect to oscillatory modulations of the volume fractions of the ions at the so-called λ -line on the $(\bar{\zeta}, T^*)$ diagram. The λ -line marks the boundary of stability of the disordered phase with respect to mesoscopic fluctuations of the volume fractions and separates the phase space into regions corresponding to the homogeneous and inhomogeneous (on the mesoscopic length scale) phases. Thus, in MF the λ -line is interpreted as a continuous order-disorder transition. In order to get the λ -line, one should solve the system of equations

$$\begin{aligned} \det \tilde{\mathbf{C}}^{MF}(k_0) &= 0, \\ \left. \frac{d \det \tilde{\mathbf{C}}^{MF}}{dk} \right|_{k=k_0} &= 0. \end{aligned}$$

When the λ -line is crossed, the inhomogeneities in the distribution of ions occur on the length scale $2\pi/k_0$. In our model, k_0 depends in particular on ϵ_{++}^* that we left as a free parameter. In order to fit ϵ_{++}^* to our water-in-salt system, we need to have $2\pi/k_0 \approx 4$ in a units ($k_0 \approx 1.6$ in a^{-1} units), for the molarity $M \sim 3 - 5$ for which the experimental data were obtained. The volume fraction of the spherical ions with $\sigma_+ = 0.2nm$ and $\sigma_- = 0.6nm$ is related to the molarity M by $\bar{\zeta}/M = \frac{\pi}{6}(0.2^3 + 0.6^3)10^{-24}N_A$, where N_A is the Avogadro number. We get $\bar{\zeta} \approx 0.27$ and $\bar{\zeta} \approx 0.32$ for the $3.8M$ and $4.6M$ systems, respectively. However, the above formula is a very rough estimation for $\bar{\zeta}/M$ in view of the strong dependence of $\bar{\zeta}$ on the diameter of the ions and the ellipsoidal shape of the TFSI⁻ anions, and it only gives the order of magnitude of M in the experimental system for given $\bar{\zeta}$ in our theory. Thus, in our semiquantitative analysis, we will consider volume fractions up to $\bar{\zeta} = 0.55$.

The plot of k_0 as a function of ϵ_{++}^* for $\epsilon_{--}^* = 1$, $\delta = 0.5$ and $\bar{\zeta} = 0.45$ is shown in Fig. 2. We can see that for $\epsilon_{++}^* = 5$, the length scale of inhomogeneities is $2\pi/k_0 \approx 3.9$ (in a -units), which for $a = 0.4nm$ gives $1.56nm$ that is close to the experimental result $1.4nm$. We thus choose $\epsilon_{++}^* = 5$ in our further calculations.

Fig. 3 shows the λ -line in the $\bar{\zeta}-T^*$ (panel a) and $\bar{\zeta}-k_0$ (panel b) coordinates for the

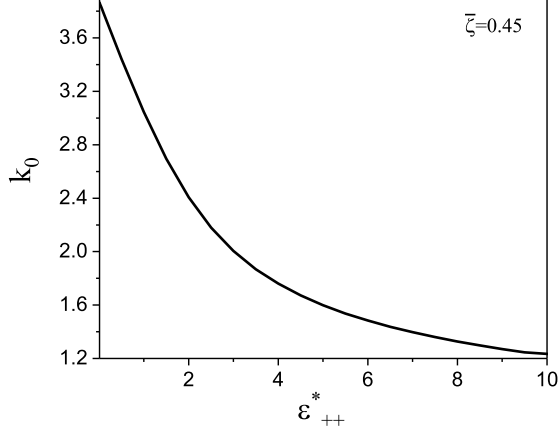


FIG. 2: The wavenumber of the density waves k_0 (in a^{-1} units) as a function of ϵ_{++}^* for $\epsilon_{--}^* = 1$, $\delta = 0.5$ and the volume fraction of ions $\bar{\zeta} = 0.45$. $\epsilon_{\alpha\alpha}^*$ describes the strength of the non-Coulombic interactions (see (6)), and the size asymmetry δ is defined in (7). For the considered system, $a = (\sigma_+ + \sigma_-)/2 \approx 0.4nm$.

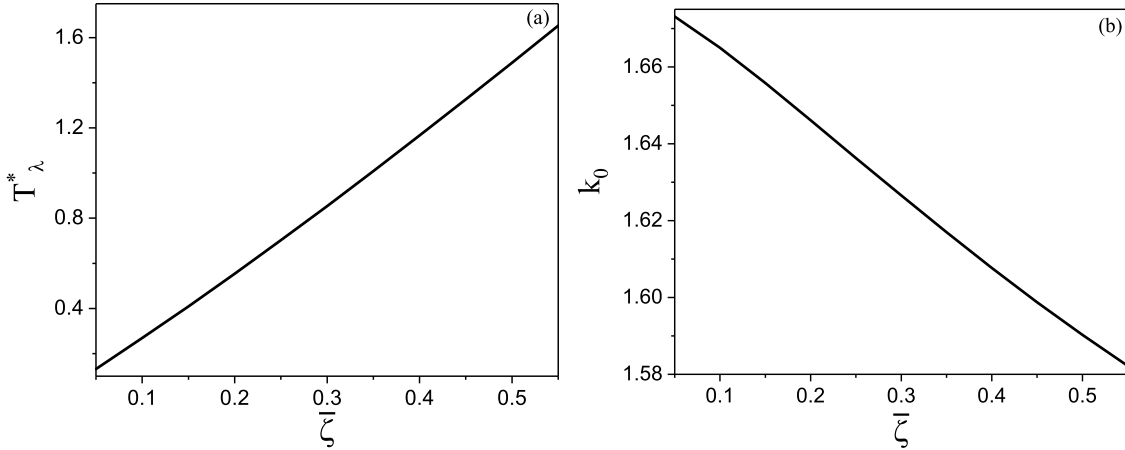


FIG. 3: λ -line in $\bar{\zeta}-T^*$ (panel a) and $\bar{\zeta}-k_0$ (panel b) coordinates for the model with $\delta = 0.5$, $\epsilon_{++}^* = 5.0$, and $\epsilon_{--}^* = 1.0$. T^* and δ are defined in (5) and (7), respectively. $\bar{\zeta} = \bar{\zeta}_+ + \bar{\zeta}_-$ is the total volume fraction of ions, $\bar{\zeta}_\alpha = \pi\rho_\alpha\sigma_\alpha^3/6$, k_0 is in the a^{-1} units, $a = (\sigma_+ + \sigma_-)/2 \approx 0.4nm$.

model with $\delta = 0.5$, $\epsilon_{++}^* = 5$, and $\epsilon_{--}^* = 1$. For the thermodynamic states below the λ -line, the waves with the wavelength $2\pi/k_0$ are more probable than the constant volume fractions. For our model, the emergence of the inhomogeneous structure for $\det \tilde{\mathbf{C}}^{MF}(k_0) < 0$ may be associated with the formation of aggregates such as clusters or layers, rather than with a phase transition. For such thermodynamic states the fluctuations dominating on the mesoscopic length scale should be taken into account in order to restore the stability of the

disordered phase. As found in different systems with spontaneously appearing mesoscopic inhomogeneities, fluctuations induce a change of the continuous transition found in MF to the first-order crystallization that is also shifted to higher volume fractions. Because of the instability of the disordered phase for $T^* < T_\lambda^*$ in MF, the asymptotic decay of the correlation functions $G_{\alpha\beta}^{MF}(r)$ can be analyzed only for $T^* > T_\lambda^*$.

In general, the long-range behaviour ($r \gg 1$) of $G_{\alpha\beta}(r)$ is described by the function [41]

$$G_{\alpha\beta}(r) = \mathcal{A}_{\alpha\beta} e^{-\alpha_0 r} \sin(\alpha_1 r + \theta_{\alpha\beta})/r. \quad (20)$$

In (20), $\alpha_0 = 1/\lambda_s$ and $\alpha_1 = 2\pi/\lambda$ are the imaginary and real parts of the leading order pole of $\tilde{G}_{\alpha\beta}(q)$ in the complex q -plane, which is determined as the complex root $q = i\alpha_0 \pm \alpha_1$ of the equation $\det \tilde{\mathbf{C}}(q) = 0$ having the smallest imaginary part. Since all $\tilde{G}_{\alpha\beta}(q)$ have a common denominator $\det \tilde{\mathbf{C}}(q)$, they exhibit the same pole structure and have the same exponential contributions. Only the amplitudes $\mathcal{A}_{\alpha\beta}$ and the phases $\theta_{\alpha\beta}$ differ for different $\alpha\beta$ combinations.

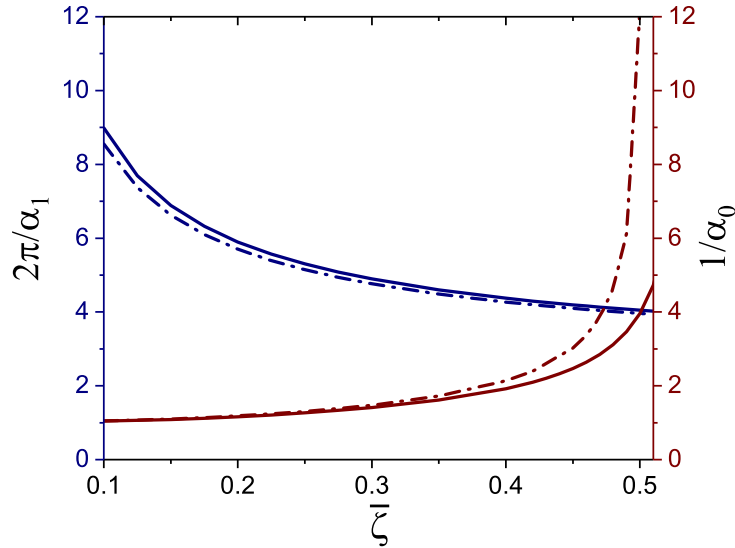


FIG. 4: (Colour online) The model with $\delta = 0.5$, $\epsilon_{++}^* = 5.0$, and $\epsilon_{--}^* = 1.0$. The decay length $\lambda_s = \alpha_0^{-1}$ and the period of oscillations $\lambda = 2\pi/\alpha_1$ of the correlation functions $G_{\alpha\beta}(r)$ as functions of the total volume fraction of ions $\bar{\zeta}$ for $T^* = 1.5$ (solid line) and $T^* = 1.6$ (dash-dotted line) in the MF approximation. α_0 and α_1 are in the a^{-1} units, with $a = (\sigma_+ + \sigma_-)/2 \approx 0.4nm$.

We calculate α_0 and α_1 for our model in MF from the equation $\det \tilde{\mathbf{C}}^{MF}(q) = 0$. The $\bar{\zeta}$ -dependence of both, the decay length $\lambda_s = \alpha_0^{-1}$ and the period of oscillations $\lambda = 2\pi/\alpha_1$

of the correlation functions $G_{\alpha\beta}(r)$ is presented in Fig. 4 for two values of the reduced temperature, $T^* = 1.5$ and $T^* = 1.6$ ($T^* > T_\lambda^*$). Note that the decay length α_0^{-1} tends to ∞ ($\alpha_0 \rightarrow 0$) and simultaneously the period of oscillations λ tends to $2\pi/k_0 \approx 4a$ when $T^* \rightarrow T_\lambda^*$. More precisely, we get $\lambda = 3.96a$ for $T^* = 1.5$, $\bar{\zeta} = 0.5$ and $\lambda = 3.98a$ for $T^* = 1.6$, $\bar{\zeta} = 0.55$.

There is a very small difference between the values of λ obtained for the two temperatures and the difference decreases with an increase of $\bar{\zeta}$. Moreover, for $\bar{\zeta} > 0.3$ the dependence of λ on $\bar{\zeta}$ is weak, as in [4].

The values of the reduced temperature $T^* > T_\lambda^*$ for large $\bar{\zeta}$, however, are too high when compared to room temperature. A rough estimate of the reduced temperature that corresponds to the conditions for the LiTFSI salt in water at room temperature ($T = 300^\circ\text{C}$ and $\varepsilon = 80$) is about 0.5. Assuming that the dielectric constant of bulk water is decreased proportionally to the ion concentration, we should consider $T^* < 0.5$.

B. Beyond the MF approximation

In order to calculate the fluctuation contribution to the inverse correlation functions $\tilde{C}_{\alpha\beta}(k)$ in the Brazovskii-type approximation, we take into account the last term in (11) and solve the closed set of four equations for the unknowns k_0 and $\tilde{C}_{\alpha\beta}(k_0)$. The explicit forms of these equations are given in Appendix D. Once k_0 and $\tilde{C}_{\alpha\beta}(k_0)$ are determined, the inverse correlation functions $\tilde{C}_{\alpha\beta}(k)$ can be obtained from Eqs. (18)–(19).

From $\mathbf{G} = \mathbf{C}^{-1}$, one can calculate the correlation functions in Fourier representation. In Fig. 5, we show the reduced correlation functions in Fourier representation $\tilde{G}_{\alpha\beta}^*(k) = \tilde{G}_{\alpha\beta}(k)/\bar{\zeta}_\alpha\bar{\zeta}_\beta$ for the fixed total volume fraction $\bar{\zeta} = 0.55$ and for two temperatures, $T^* = 0.25$ (panel a) and $T^* = 0.2$ (panel b). The three correlation functions $\tilde{G}_{\alpha\beta}^*(k)$ have sharp maxima for $k = k_0 \simeq 1.58$. For both temperatures the height of the $\tilde{G}_{++}^*(k)$ maximum is about 100 times higher than the maximum of $\tilde{G}_{--}^*(k)$. It should be noted that the dependence of k_0 on T^* for the fixed $\bar{\zeta}$ is negligible, especially in the range $T^* = 0.2 - 0.3$ (see Table I).

The reduced correlation functions in real-space representation, $G_{\alpha\beta}^*(r) = G_{\alpha\beta}(r)/\bar{\zeta}_\alpha\bar{\zeta}_\beta$, are obtained from the inverse Fourier transformation of $\tilde{G}_{\alpha\beta}^*(k)$. They are shown in Fig. 6 for $T^* = 0.25$, $\bar{\zeta} = 0.55$ (panel a) and for $T^* = 0.2$, $\bar{\zeta} = 0.55$ (panel b). As it is seen, $G_{\alpha\beta}^*(r)$ show exponentially damped oscillatory behavior described by (20). The period of damped

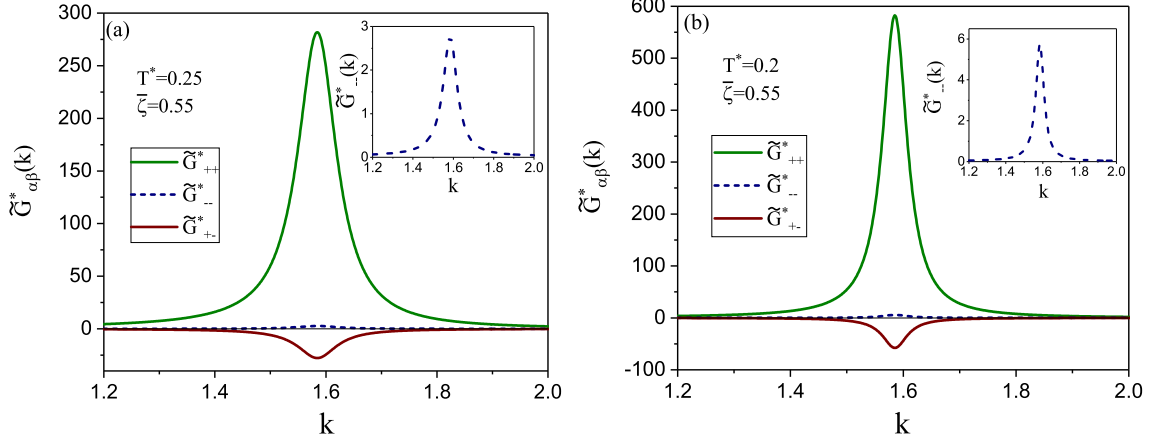


FIG. 5: Correlation functions in Fourier representation with the effect of fluctuations taken into account for $T^* = 0.25$, $\bar{\zeta} = 0.55$ (panel a) and for $T^* = 0.2$, $\bar{\zeta} = 0.55$ (panel b). $\tilde{G}_{\alpha\beta}^* = \tilde{G}_{\alpha\beta} / \bar{\zeta}_\alpha \bar{\zeta}_\beta$, $\bar{\zeta}_\alpha = \pi \rho_\alpha \sigma_\alpha^3 / 6$, and the wave number k is in a^{-1} units with $a = (\sigma_+ + \sigma_-) / 2$. The results are for the model with $\delta = 0.5$, $\epsilon_{++}^* = 5$, $\epsilon_{+-}^* = 1$. In the insets, we show sharp peaks of $\tilde{G}_{--}^*(k)$.

TABLE I: The wave number k_0 , the decay length α_0^{-1} and the period of oscillations $\lambda = 2\pi / \alpha_1$ of the pair correlation functions $G_{\alpha\beta}(r)$ depending on the total number density $\bar{\zeta}$ for fixed values of temperature T^* . T^* is defined in (5), $\bar{\zeta} = \bar{\zeta}_+ + \bar{\zeta}_-$, $\bar{\zeta}_\alpha = \pi \rho_\alpha \sigma_\alpha^3 / 6$, k_0 , α_0 and α_1 are in a^{-1} units.

T^*	$\bar{\zeta}$	k_0	α_0	α_1	α_0^{-1}	$2\pi / \alpha_1$
0.4	0.45	1.597	0.225	1.613	4.444	3.895
0.4	0.5	1.591	0.163	1.599	6.151	3.930
0.4	0.55	1.582	0.119	1.587	8.424	3.959
0.3	0.45	1.602	0.124	1.607	8.042	3.910
0.3	0.5	1.593	0.088	1.595	11.426	3.939
0.3	0.55	1.584	0.063	1.585	15.796	3.964
0.25	0.45	1.605	0.084	1.607	11.852	3.911
0.25	0.5	1.594	0.059	1.595	16.920	3.939
0.25	0.55	1.584	0.043	1.585	23.411	3.964
0.2	0.45	1.607	0.053	1.608	19.016	3.907
0.2	0.5	1.595	0.037	1.596	27.191	3.937
0.2	0.55	1.585	0.027	1.585	37.610	3.963

oscillations is about $4a$. We study the asymptotic decay of the correlation functions $G_{\alpha\beta}(r)$ using the pole analysis. The results of this numerical analysis for $T^* = 0.2, 0.25, 0.3,$ and 0.4 and for $\bar{\zeta} = 0.45, 0.5, 0.55$ are summarized in Table I. For the fixed volume fraction, the period $\lambda = 2\pi/\alpha_1$ coincides with $2\pi/k_0$ and is rather kept constant for $T^* \leq 0.3$. For the fixed temperature, λ is a weakly increasing function of $\bar{\zeta}$. It should be noted that the period of damped oscillations obtained with the effect of fluctuations taken into account is very close to the period obtained in MF for the higher temperature. By contrast, the decay length α_0^{-1} noticeably increases with an increase of $\bar{\zeta}$ for the fixed temperature and this increase is more rapid for lower temperatures. In Fig. 7, we present the decay length α_0^{-1} as a function of the total volume fraction of ions $\bar{\zeta}$ for fixed temperatures (panel a) and as a function of the Bjerrum length l_B for fixed volume fractions (panel b). One can observe that α_0^{-1} has a nearly linear dependence on the volume fraction for fixed T^* , with the slope decreasing with T^* and a nearly linear dependence on l_B for fixed $\bar{\zeta}$, with the slope increasing with $\bar{\zeta}$.

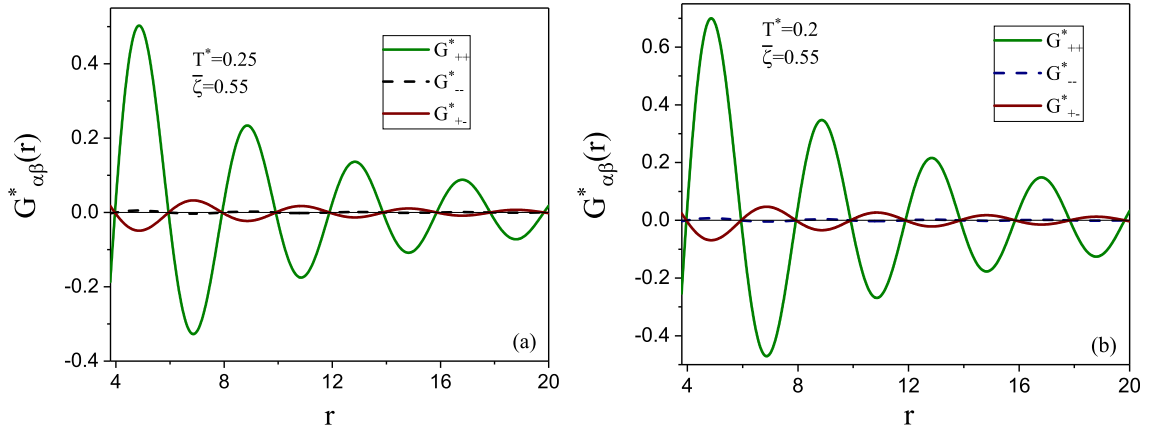


FIG. 6: Correlation functions in real space with the effect of fluctuations taken into account for $\bar{\zeta} = 0.55$, $T^* = 0.25$ (panel a) and $T^* = 0.2$ (panel b). $G_{\alpha\beta}^* = G_{\alpha\beta}/\bar{\zeta}_\alpha\bar{\zeta}_\beta$, $\bar{\zeta}_\alpha = \pi\rho_\alpha\sigma_\alpha^3/6$, and r is in a units with $a = (\sigma_+ + \sigma_-)/2$. The results are for the model with $\delta = 0.5$, $\epsilon_{++}^* = 5$, $\epsilon_{+-}^* = 1$.

V. SUMMARY AND CONCLUSIONS

We have developed a highly simplified model for water-in-salt electrolytes, and focused on the salt LiTFSI that was a subject of recent experiments [3, 4]. In our model, the ions

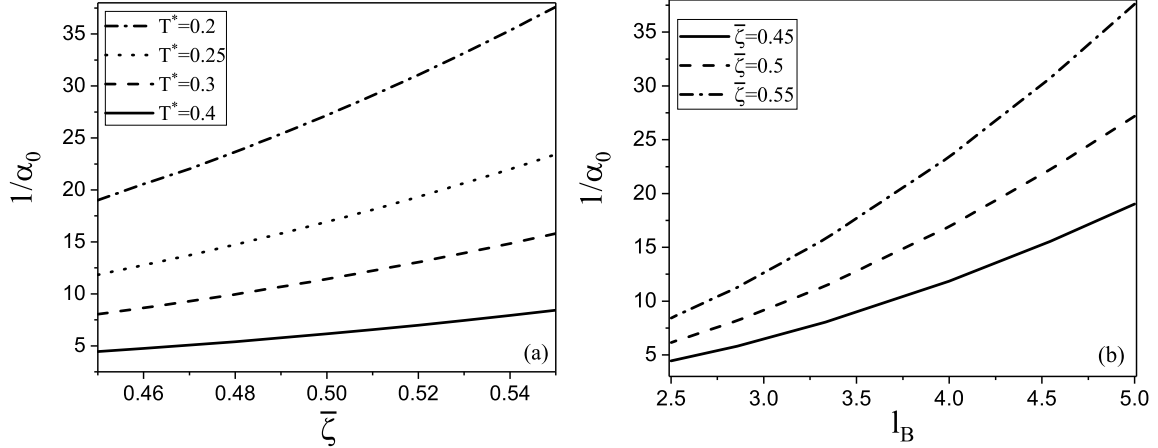


FIG. 7: The decay length α_0^{-1} of the correlation functions $G_{\alpha\beta}(r)$ as a function of the total volume fraction of ions $\bar{\zeta}$ for $T^* = 0.2, 0.25, 0.3, 0.4$ (from the top to the bottom line) (panel a) and as a function of the Bjerrum length l_B for $\bar{\zeta} = 0.45, 0.5, 0.55$ (from the bottom to the top line) (panel b). $1/\alpha_0$ and l_b are in the a units, $a = (\sigma_+ + \sigma_-)/2 \approx 0.4nm$. The results are for the model with $\delta = 0.5$, $\epsilon_{++}^* = 5$, $\epsilon_{++}^* = 1$.

are treated as charged hard spheres with different diameters, and we assumed additional, water-mediated specific interactions between the ions of the same sign. We assumed that the solvent influences the distribution of the ions mainly by inducing effective interactions between them, and otherwise the solvent can be neglected. Next, we assumed that the detailed shape of the specific interactions is not important, as long as these interactions are strongly attractive but of a short range. We chose the Yukawa potentials for the specific interactions, and adjusted the parameters to the LiTFSI by requiring the same scale of inhomogeneities as found experimentally. Importantly, the obtained sum of the Coulomb and specific interactions for both, the anions and the cations is attractive at short- and repulsive at large distances.

For this model, we calculated correlation functions for concentrated electrolytes for reduced temperatures close to the room temperature, using our theory for binary mixtures with competing interactions [32, 33, 37]. There is no unique way of relating the volume fraction in the approximate theory to experimental molarity, since we assumed spherical rather than ellipsoidal anions, and the values of the ion diameters in the theory are not precise. We considered volume fractions $0.45 \leq \bar{\zeta} \leq 0.55$ somewhat larger than in the experiment,

but of the same order of magnitude (the molarity $0.38 - 0.46$ considered in [4] for spherical ions of our sizes gives $0.27 \leq \bar{\zeta} \leq 0.32$). We obtained exponentially damped oscillations for the correlation functions with the period $\lambda \approx 4$ in $a \approx 0.4nm$ -units (in the experiment [3, 4], $\lambda \approx 1.4nm$), very weakly depending on $\bar{\zeta}$ in the considered range of concentrations. In MF, λ decreases a bit, whereas when the fluctuations are taken into account, it a bit increases with $\bar{\zeta}$. Interestingly, λ slightly decreases, increases or does not change with increasing $\bar{\zeta}$, depending on the method of determining it in the experiment [4].

We found that the decay length of the correlations, λ_s , increases almost linearly with $\bar{\zeta}$ for fixed reduced temperature T^* . It increases also with the Bjerrum length for temperatures of the order of the room temperature. In particular, for the reduced temperature $T^* = 0.3$ (Bjerrum length $l_B = 3.3$ in $a \approx 0.4nm$ units), we obtain $\lambda_s \approx 3.2 - 6nm$, and for $T^* = 0.2$ (Bjerrum length $l_B = 5$) we obtain $\lambda_s \approx 8 - 15nm$ for $\bar{\zeta} = 0.45 - 0.55$. These values are in semiquantitative agreement with the experimental decay lengths, $\lambda_s = 8.3 - 11.5nm$ for the molarity $3.8 - 4.6M$ ($\bar{\zeta} = 0.27 - 0.32$).

The very weak dependence of λ on $\bar{\zeta}$ and the semiquantitative agreement of the decay length with the experimental results indicate that the properties of the correlation functions do not depend sensitively on the details of the interactions. The ellipsoidal anions are approximated by the spherical ones, implicit solvent inducing effective anion-anion and cation-cation interactions is assumed, and we neglected fluctuations of the dielectric constant induced by the concentration fluctuations. The dependence of the reduced temperature on $\bar{\zeta}$ (through the dependence of ϵ on $\bar{\zeta}$) was disregarded as well. The latter dependence for the rather narrow range of $\bar{\zeta}$ is not very strong, however. Finally, we rather arbitrarily assumed the shape of the specific interactions. With the above simplifications, we got semiquantitative agreement with experiments. It means that the above features are important only on the quantitative level.

We conclude that the key property determining the inhomogeneities on the mesoscopic length scale is the shape of the sum of the Coulomb and the solvent-induced specific interactions. In order to induce mesoscopic inhomogeneities, this sum should be attractive at short- and repulsive at large distances, with the ranges and strengths of the attractive and repulsive parts determined by the properties of the ions and the solvent. If these anion-anion and cation-cation potentials have a negative minimum followed by a positive maximum, then layers of ions of the same sign of the thickness determined by the width and depth of

the attractive well can be formed. We believe that this conclusion is not restricted to the particular case of the water-in-LiTFSI, but rather general.

Finally, we have shown that the self-consistent theory with the local fluctuations of the volume fractions taken into account [32, 33] can predict the structure with local inhomogeneities on a semiquantitative level.

There remains one unsolved problem - namely, the experimental disjoining pressure between crossed mica cylinders decays monotonically at large distances [4], whereas our theory predicts the oscillatory decay. The same problem concerns simple salts and some other IL modeled by the RPM.

VI. APPENDICES

A. Interaction potentials in Fourier representation

The interaction potentials $\beta\tilde{U}_{\alpha\beta}^C$ and $\beta\tilde{U}_{\alpha\alpha}^A$ (see (2)–(6)) in Fourier representation read

$$\beta\tilde{U}_{++}^C(k) = \frac{4\pi \cos(k(1-\delta))}{T^* k^2}, \quad (21)$$

$$\beta\tilde{U}_{--}^C(k) = \frac{4\pi \cos(k(1+\delta))}{T^* k^2}, \quad (22)$$

$$\beta\tilde{U}_{+-}^C(k) = -\frac{4\pi \cos(k)}{T^* k^2}, \quad (23)$$

$$\beta\tilde{U}_{++}^A(k) = -\frac{4\pi\epsilon_{++}^*(1-\delta)}{T^*(z^2+k^2)} \left[\cos(k(1-\delta)) + \frac{z}{k} \sin(k(1-\delta)) \right], \quad (24)$$

$$\beta\tilde{U}_{--}^A(k) = -\frac{4\pi\epsilon_{--}^*(1+\delta)}{T^*(z^2+k^2)} \left[\cos(k(1+\delta)) + \frac{z}{k} \sin(k(1+\delta)) \right], \quad (25)$$

where z and k are in a^{-1} units.

B. Free-energy density for a mixture of hard spheres with different diameters

For the free energy density βf_{hs} we use the expression obtained in the Carnahan-Starling approximation [42]

$$\beta f_{hs} = \frac{6}{\pi(1-\delta^2)^3} [\zeta_+(1+\delta)^3 + \zeta_-(1-\delta)^3] \left[-\frac{3}{2}(1-y_1+y_2+y_3) + \frac{3y_2+2y_3}{1-\zeta} + \frac{3(1-y_1-y_2-y_3/3)}{2(1-\zeta)^2} + (y_3-1)\ln(1-\zeta) \right],$$

with

$$\begin{aligned}
y_1 &= \frac{8\delta^2\zeta_+\zeta_-}{\zeta[\zeta_+(1+\delta)^3 + \zeta_-(1-\delta)^3]}, \\
y_2 &= \frac{4\delta^2\zeta_+\zeta_-}{\zeta^2} \frac{[\zeta_+(1+\delta) + \zeta_-(1-\delta)]}{[\zeta_+(1+\delta)^3 + \zeta_-(1-\delta)^3]}, \\
y_3 &= \frac{[\zeta_+(1+\delta) + \zeta_-(1-\delta)]^3}{\zeta^2[\zeta_+(1+\delta)^3 + \zeta_-(1-\delta)^3]},
\end{aligned}$$

C. Expressions for $\tilde{C}^{MF}(k)$

Taking into account (21)-(25), (8), and (12), the matrix \tilde{C}^{MF} can be presented as follows:

$$\begin{aligned}
\tilde{C}_{++}^{MF}(k) &= \frac{144 \cos(k(1-\delta))}{T^*\pi(1-\delta)^6 k^2} - \frac{144\epsilon_{++}^*}{T^*\pi(1-\delta)^5(z^2+k^2)} \left[\cos(k(1-\delta)) \right. \\
&\quad \left. + \frac{z}{k} \sin(k(1-\delta)) \right] + A_{++}, \tag{26}
\end{aligned}$$

$$\begin{aligned}
\tilde{C}_{--}^{MF}(k) &= \frac{144 \cos(k(1+\delta))}{T^*\pi(1+\delta)^6 k^2} - \frac{144\epsilon_{--}^*}{T^*\pi(1+\delta)^5(z^2+k^2)} \left[\cos(k(1+\delta)) \right. \\
&\quad \left. + \frac{z}{k} \sin(k(1+\delta)) \right] + A_{--}, \tag{27}
\end{aligned}$$

$$\tilde{C}_{+-}^{MF}(k) = -\frac{144 \cos(k)}{T^*\pi(1-\delta^2)^3 k^2} + A_{+-}, \tag{28}$$

where

$$A_{\alpha\beta} = \frac{6}{\pi} \frac{\delta_{\alpha\beta}}{\zeta_\alpha a_\alpha^3} + \frac{\partial^2 \beta f_{hs}}{\partial \zeta_\alpha \partial \zeta_\beta}, \quad a_\pm = 1 \mp \delta. \tag{29}$$

D. Equations for k_0 and $\tilde{C}_{\alpha\beta}(k_0)$ in our mesoscopic theory.

The equations to be solved for k_0 and $\tilde{C}_{\alpha\beta}(k_0)$ are (see sec.III and Ref.[32])

$$\begin{aligned}
&\tilde{V}'_{++}(k_0)\tilde{C}_{--}(k_0) + \tilde{V}'_{--}(k_0)\tilde{C}_{++}(k_0) - 2\tilde{V}'_{+-}(k_0)\tilde{C}_{+-}(k_0) = 0, \\
\tilde{C}_{++}(k_0) &= \tilde{C}_{++}^{MF}(k_0) + \frac{k_0^2}{2\pi[2\beta\tilde{W}''(k_0)D_0]^{1/2}} \left[A_{++++}\tilde{C}_{--}(k_0) - 2A_{++++}\tilde{C}_{+-}(k_0) \right. \\
&\quad \left. + A_{+---}\tilde{C}_{++}(k_0) \right], \\
\tilde{C}_{--}(k_0) &= \tilde{C}_{--}^{MF}(k_0) + \frac{k_0^2}{2\pi[2\beta\tilde{W}''(k_0)D_0]^{1/2}} \left[A_{+---}\tilde{C}_{--}(k_0) - 2A_{+---}\tilde{C}_{+-}(k_0) \right. \\
&\quad \left. + A_{----}\tilde{C}_{++}(k_0) \right], \\
\tilde{C}_{+-}(k_0) &= \tilde{C}_{+-}^{MF}(k_0) + \frac{k_0^2}{2\pi[2\beta\tilde{W}''(k_0)D_0]^{1/2}} \left[A_{++++}\tilde{C}_{--}(k_0) - 2A_{+---}\tilde{C}_{+-}(k_0) \right. \\
&\quad \left. + A_{+---}\tilde{C}_{++}(k_0) \right].
\end{aligned}$$

where

$$\beta W''(k_0) = 2\beta^2 \det \mathbf{V}' + \beta \tilde{V}_{++}'' \tilde{C}_{--}(k_0) + \beta \tilde{V}_{--}'' \tilde{C}_{++}(k_0) - 2\beta \tilde{V}_{+-}'' \tilde{C}_{+-}(k_0), \quad (30)$$

with $\tilde{V}'_{\alpha\beta}(k_0) = d\tilde{V}_{\alpha\beta}(k)/dk|_{k=k_0}$, $\tilde{C}_{\alpha\beta}^{MF}(k_0)$ are obtained from (26)- (29) by putting $k = k_0$, D_0 is presented in (17), and

$$A_{\alpha\beta\gamma\delta} = \frac{12}{\pi} \frac{\delta_{\alpha\beta} \delta_{\alpha\gamma} \delta_{\alpha\delta}}{\zeta_{\alpha}^3 a_{\alpha}^3} + \frac{\partial^4 \beta f_{hs}}{\partial \zeta_{\alpha} \partial \zeta_{\beta} \partial \zeta_{\gamma} \partial \zeta_{\delta}}. \quad (31)$$

-
- [1] M. Chen, G. Feng, and R. Qiao, *Current Opinion in Colloid & Interface Science* **47**, 99 (2020).
- [2] L. Suo, O. Borodin, T. Gao, M. Olguin, J. Ho, X. Fan, C. Luo, C. Wang, and K. Xu, *Science* **350**, 938 (2015).
- [3] O. Borodin, L. Suo, M. Gobet, X. Ren, F. W. A. Faraone, J. Peng, M. Olguin, M. Schroeder, M. S. Ding, E. Gobrogge, et al., *ACS Nano* **11**, 10462 (2017).
- [4] T. S. Groves, C. S. Perez-Martinez, R. Lhermerout, and S. Perkin, *J. Phys. Chem. Lett.* **12**, 1702 (2021).
- [5] M. A. Gebbie, M. Valtiner, X. Banquy, E. T. Fox, W. A. Henderson, and J. N. Israelachvili, *Proc. Nat. Acad. Sci. USA* **110**, 9674 (2013).
- [6] A. M. Smith, A. A. Lee, and S. Perkin, *J. Phys. Chem. Lett.* **7**, 2157 (2016).
- [7] A. Lee, C. S. Perez-Martinez, A. M. Smith, and S. Perkin, *Phys. Rev. Lett.* **119**, 026002 (2017).
- [8] R. Kjellander, *J. Chem. Phys.* **148**, 193701 (2018).
- [9] R. Kjellander, *Soft Matter* **15**, 5866 (2019).
- [10] Z. A. Goodwin and A. A. Kornyshev, *Electrochemistry Communications* **82**, 129 (2017).
- [11] N. B. Ludwig, K. Dasbiswas, D. V. Talapin, and S. Vaikuntanathan, *J. Chem. Phys.* **149**, 164505 (2018).
- [12] B. Rotenberg, O. Bernard, and J.-P. Hansen, *J. Phys.: Condens. Matter* **30**, 054005 (2018).
- [13] R. M. Adar, S. A. Safran, H. Diamant, and D. Andelman, *Phys. Rev. E* **100**, 042615 (2019).
- [14] J. P. de Souza, Z. A. Goodwin, M. McEldrew, A. A. Kornyshev, and M. Z. Bazant, *Phys. Rev. Lett.* **125**, 116001 (2020).
- [15] C. W. Outhwaite and L. B. Bhuiyan, *J. Chem. Phys.* **155**, 014504 (2021).

- [16] S. W. Coles, C. Park, R. Nikam, M. Kanduč, J. Dzubiella, and B. Rotenberg, *J. Phys. Chem. B* **124**, 1778 (2020).
- [17] J. Zeman, S. Kondrat, and C. Holm, *Chem. Comm.* **56**, 15635 (2020).
- [18] A. Ciach and O. Patsahan, *J. Phys.: Condens. Matter* **33**, 37LT01 (2021).
- [19] G. Stell, *J. Stat. Phys.* **78**, 197 (1995).
- [20] M. E. Fisher, *J. Stat. Phys.* **75**, 1 (1994).
- [21] R. L. de Carvalho and R. Evans, *Mol. Phys* **83**, 619 (1994).
- [22] A. Ciach, W. T. Gózdź, and R. Evans, *J. Chem. Phys.* **118**, 3702 (2003).
- [23] J.G.Kirkwood, *Chem.Rev.* **19**, 275 (1936).
- [24] M. V. Fedorov and A. A. Kornyshev, *J. Phys. Chem. B* **112**, 11868 (2008).
- [25] M. V. Fedorov and A. A. Kornyshev, *Chem. Rev.* **114**, 2978 (2014).
- [26] O. Patsahan and A. Ciach, *J. Phys.: Condens. Matter* **19**, 236203 (2007).
- [27] A. Ciach and G. Stell, *J. Chem. Phys.* **114**, 382 (2001).
- [28] A. Ciach, W. T. Gózdź, and G. Stell, *Phys. Rev. E* **75**, 051505 (2007).
- [29] O. V. Patsahan and T. M. Patsahan, *Phys. Rev. E* **81**, 031110 (2010).
- [30] O. V. Patsahan and T. M. Patsahan, *J. Mol. Liq.* **164**, 44 (2011).
- [31] O. Patsahan and A. Ciach, *Phys. Rev. E* **86**, 031504 (2012).
- [32] A. Ciach, O. Patsahan, and A. Meyra, *Condens. Matter Phys.* **23**, 23601 (2020).
- [33] O. Patsahan, A. Meyra, and A. Ciach, *Mol. Phys.* **119**, 1820091 (2021).
- [34] A. de Candia, E. D. Gado, A. Fierro, N. Sator, M. Tarzia, and A. Coniglio, *Phys. Rev. E* **74**, 010403(R) (2006).
- [35] A. J. Archer and N. B. Wilding, *Phys. Rev. E* **76**, 031501 (2007).
- [36] A. Ciach, J. Pękałski, and W. T. Gózdź, *Soft Matter* **9**, 6301 (2013).
- [37] A. Ciach, *Mol. Phys* **109**, 1101 (2011).
- [38] S. A. Brazovskii, *Sov. Phys. JETP* **41**, 85 (1975).
- [39] A. Ciach and O. Patsahan, *Condens. Matter Phys.* **15**, 23604 (2012).
- [40] O. Patsahan, M. Litniewski, and A. Ciach, *Soft Matter* **17**, 2883 (2021).
- [41] R. Evans, R. L. de Carvalho, J. R. Henderson, and D. C. Hoyle, *J. Chem. Phys.* **100**, 591 (1994).
- [42] G. Mansoori, N. F. Carnahan, K. E. Starling, and J. T. W. Leland, *J. Chem. Phys.* **54**, 1523 (1971).